

Supplementary materials

Analysis of the effect of abiotic stressors on BVOC emissions from urban green infrastructure in northern Germany

J. Feldner^a, M. Ramacher^a, M. Karl^{*a}, M. Quante^a, and M. L. Luttkus^b

^a Helmholtz Centre Hereon, Max-Planck-Str. 2, 21502 Geesthacht, Germany.

^b Leibniz Institute for Tropospheric Research e.V. (TROPOS), Permoserstr. 15, 04318 Leipzig, Germany.

* Correspondence: matthias.karl@hereon.de

Supplement S1 – Description of anthropogenic emissions in the EPISODE-CityChem setup

To account for industrial point sources a dataset from the Behörde für Umwelt, Klima, Energie und Agrarwirtschaft (BUKEA), formerly known as Behörde für Umwelt und Energie was used. This data accounts mainly for facilities subject to mandatory permission under the 11th Bundesimmisionsschutzverordnung (BImSchV) reported in the year 2016 in Hamburg. Besides exact locations, the applied dataset contains information about annual emission totals for different pollutants and several stack parameters (stack height, exit velocity and temperature) for each of the 746 reported stacks. In addition, we included emissions from road traffic of the highway in the Elbe Tunnel, which are routed to the surface via two central ventilation systems, in the inventory of point sources and removed them from the inventory of line sources accordingly.

Land-based emissions for commercial and industrial combustion processes, domestic heating, road traffic, agriculture, waste and solvent emissions are preprocessed with the UrbEm framework, which is a hybrid method to derive high-resolved emissions for city-scale air quality modelling studies (Ramacher et al., 2021). An exception in the industrial sector are sources that have been classified as point sources (see above). In the UrbEm framework regional-scale area emissions of the CAMS 2016 REG-AP v3.1 regional emission inventory (Kuenen et al., 2021) are downscaled to the urban-scale domain definition in this study under application of sector-specific proxies, given in Ramacher et al. (2021). The result of this approach are a detailed line source emission inventory (based on OpenStreetMap road networks) for road traffic and a 1 km grid emission inventory for area emissions of the remaining sectors.

To achieve annual emissions for the shipping sector, a bottom-up ship emission modeling system (MoSES, Schwarzkopf et al. 2021) was applied for the year 2018. The emission calculation in MoSES is based on information about the ship (e.g. ship type, fuel type, engine power). Navigational information like speed and location as well as ship identification data are transferred as AIS data. MoSES enables differentiation between the use of main and auxiliary engines; the latter is important for berthing ships.

The annual totals of all anthropogenic emission sectors in the EPISODE-CityChem domain are then temporally disaggregated using the Urban Emission Conversion Tool (UECT). The result of UECT are hourly emissions of each emission sector individually.

Supplement S2 – Chemical mechanism used in the EPISODE-CityChem model

The urban chemistry scheme EmChem09-HET of EPISODE-CityChem v1.5 includes 78 chemical reactions and 28 photo-dissociation reactions. Table S2-1 lists the chemical species that are included in EmChem09-HET and indicates which of the species are linked to emission input from the Model of Emissions of Gases and Aerosols from Nature (MEGAN) version 3. Table S2-2 lists the chemical reactions of isoprene, APIN and LIM in EmChem09-HET. Table S2-3 presents the mapping of chemical species from MEGAN 3 to the compounds of the urban chemistry scheme EmChem09-HET.

Table S2-1: Compounds used in CityChem chemistry mechanisms Emchem09-HET of EPISODE-CityChem v1.5 and considered BVOC species emission linkage (direct / indirect) to MEGAN 3.

Compound Name	Full name / class	anthropogenic emissions	biogenic emissions
O3	Ozone	not applicable	not applicable
NO	Nitric oxide	CAMS	not included
NO2	Nitrogen dioxide	CAMS	not included
H2O2	hydrogen peroxide		not included
N2O5	Dinitrogen pentoxide		not included
HNO3	Nitric acid		not included
HONO	Nitrous acid		not included
SO2	Sulphur dioxide	CAMS	not included
Sulphate	Sulphuric acid		not included
CO	Carbon monoxide	CAMS	not included
C2H6	Ethane	CAMS	MEGAN v3 indirect
HCHO	Formaledhyde	CAMS	MEGAN v3 indirect
CH3CHO	Acetaldehyde and higher aldehydes	CAMS	MEGAN v3 indirect
C2H4	Ethene	CAMS	MEGAN v3 indirect
PAN	Peroxy acetyl nitrate		not included
MACR	Methacrolein		not included
MPAN	Peroxy methacryloyl nitrate		not included
nC4H10	n-butane and other alkanes n>3	CAMS	MEGAN v3 indirect
CH3COC2H5	Methyl ethyl ketone (and other ketones)	CAMS	MEGAN v3 indirect
C3H6	Propene and other n>4 alkenes	CAMS	MEGAN v3 indirect
o-Xylene	o-Xylene and other aromatic HCs	CAMS	not included
Isoprene	Isoprene		MEGAN v3 direct

APIN	α -pinene and other relatively slow reacting MT		MEGAN v3 direct
LIM	Limonene and other fast reacting MT		MEGAN v3 direct
C2H5OH	Ethanol		MEGAN v3 direct
CH3OH	Methanol		MEGAN v3 direct
PM2.5	Particulate Matter	CAMS	not included
PM10	Particulate Matter	CAMS	not included

Table S2-2: Photochemical reactions of isoprene and of monoterpenes in EmChem09-HET.

ktr ($\text{CH}_3\text{OO}_2 + \text{NO}_2$): $k_0/M = 2.7\text{E}-28$ (300/T) 7.1, $k_\infty = 1.2\text{-}11$ (300/T) 0.9, $F_c = 0.3$

ktr (PAN): $k_0/M = 4.9\text{E}-3$ (300/T) -12100, $k_\infty = 5.4\text{E}16 \exp(-13830/T)$, $F_c = 0.3$

Isoprene chemistry

IS-1	$\text{C}_5\text{H}_8 + \text{OH}$	\rightarrow	ISOPO_2	$2.7\text{E}-11 \exp(390/T)$
IS-2	$\text{C}_5\text{H}_8 + \text{NO}_3$	\rightarrow	ISOPNO_3	$3.03\text{E}-12 \exp(-446/T)$
IS-3	$\text{C}_5\text{H}_8 + \text{O}_3$	\rightarrow	$0.26 \text{ MVK} + 0.39 \text{ MACR} + 0.90 \text{ HCHO} + 0.10 \text{ MVKO}_2 + \text{CH}_3\text{COO}_2 + \text{CH}_3\text{O}_2 + 0.09 \text{ H}_2\text{O}_2 + 0.25 \text{ HO}_2 + 0.25 \text{ OH}$	$7.86\text{E}-15 \exp(-1913/T)$
IS-4	$\text{ISOPO}_2 + \text{NO}$	\rightarrow	$0.34 \text{ MVK} + 0.22 \text{ MACR} + 0.34 \text{ CAR4} + 0.63 \text{ HCHO} + 0.05 \text{ ISNI} + \text{HO}_2 + \text{NO}_2$	$2.54\text{E}-12 \exp(360/T)$
IS-5	$\text{MVK} + \text{OH}$	\rightarrow	MVKO_2	$2.6\text{E}-12 \exp(610/T)$
IS-6	$\text{MACR} + \text{OH}$	\rightarrow	$0.5 \text{ MVKO}_2 + 0.5 \text{ MACO}_3$	$8.0\text{E}-12 \exp(380/T)$
IS-7	$\text{CAR4} + \text{OH}$	\rightarrow	MVKO_2	$4.52\text{E}-11$
IS-8	$\text{MVKO}_2 + \text{NO}$	\rightarrow	$\text{NO}_2 + 0.25 \text{ CH}_3\text{COCH}_2\text{OH} + 0.25 \text{ CO} + 0.5 \text{ CH}_3\text{COCHO} + 0.75 \text{ HCHO} + 0.75 \text{ HO}_2$	$2.54\text{E}-12 \exp(360/T)$
IS-9	$\text{ISOPO}_2 + \text{HO}_2$	\rightarrow	$0.857 \text{ ISRO}_2\text{H}$	$0.706 \times 2.91\text{E}-13 \exp(1300/T)$
IS-10	$\text{ISRO}_2\text{H} + \text{OH}$	\rightarrow	$\text{OH} + \text{CAR4}$	$1.00\text{E}-10$
IS-11	$\text{ISOPNO}_3 + \text{NO}$	\rightarrow	$1.1 \text{ NO}_2 + 0.8 \text{ HO}_2 + 0.85 \text{ ISNI} + 0.1 \text{ MACR} + 0.15 \text{ HCHO} + 0.05 \text{ MVK}$	$2.54\text{E}-12 \exp(360/T)$
IS-12	$\text{ISNI} + \text{OH}$	\rightarrow	$\text{CH}_3\text{COCH}_2\text{OH} + \text{NALD}$	$1.3\text{E}-11$
IS-13	$\text{MVKO}_2 + \text{HO}_2$	\rightarrow	MVKO_2H	$0.625 \times 2.91\text{E}-13 \exp(1300/T)$
IS-14	$\text{MVKO}_2\text{H} + \text{OH}$	\rightarrow	MVKO_2	$3.0\text{E}-11$
IS-15	$\text{NALD} + \text{OH}$	\rightarrow	$\text{HCHO} + \text{CO} + \text{NO}_2$	$5.6\text{E}-12 \exp(270/T)$
IS-16	$\text{MVK} + \text{O}_3$	\rightarrow	$0.90 \text{ CH}_3\text{COCHO} + 0.32 \text{ HO}_2 + 0.22 \text{ CO} + 0.19 \text{ OH} + 0.10 \text{ CH}_3\text{COO}_2$	$7.51\text{E}-16 \exp(-1521/T)$
IS-17	$\text{MACR} + \text{O}_3$	\rightarrow	$0.90 \text{ CH}_3\text{COCHO} + 0.32 \text{ HO}_2 + 0.22 \text{ CO} + 0.19 \text{ OH} + 0.10 \text{ CH}_3\text{COO}_2$	$1.36\text{E}-15 \exp(-2112/T)$

IS-18	CAR4 + O3	\rightarrow	0.90 CH3COCHO + 0.32 HO2 + 0.22 CO + 0.19 OH + 0.10 CH3COO2	2.4E-17
IS-19	MPAN + OH	\rightarrow	CH3COCH2OH + CO + NO2	2.9E-11
IS-20	MACO3 + NO	\rightarrow	CH3COO2 + HCHO + NO2	8.7E-12 exp(290/T)
IS-21	MACO3 + NO2	\rightarrow	MPAN	ktr (CH3OO2 + NO2)
IS-22	MPAN	\rightarrow	MACO3 + NO2	ktr (PAN)

Monoterpene chemistry

MT-1	APIN + OH	\rightarrow	PRODAPINOH + MTO2	1.2E-11 exp(444/T)
MT-2	APIN + NO3	\rightarrow	PRODAPINNO3 + MTO2	1.2E-12 exp(490/T)
MT-3	APIN + O3	\rightarrow	0.8 PRODAPINO3 + 0.8 MTO2 + 0.2 BLOC + 0.46 OH	6.3E-16 exp(-580/T)
MT-4	LIM + OH	\rightarrow	PRODLIMOH + MTO2	1.7E-10
MT-5	LIM + NO3	\rightarrow	PRODLIMNO3 + MTO2	1.3E-11
MT-6	LIM + O3	\rightarrow	PRODLIMO3 + 0.67 OH + 0.19 HCHO + MTO2	2.0E-16
MT-7	MTO2 + NO	\rightarrow	NO2 + HO2 + 0.78 MTKETONE	2.54E-12 exp(360/T)
MT-8	MTO2 + HO2	\rightarrow	0.493 MTO2H	$0.914 \times 2.91E-13$ exp(1300/T)
MT-9	MTO2 + CH3O2	\rightarrow	MTO2H	2.91E-13 exp(1300/T)
MT-10	MTO2 + C2H5O2	\rightarrow	MTO2H	2.91E-13 exp(1300/T)
MT-11	PRODAPINOH + OH	\rightarrow	MTO2	1.0E-30
MT-12	PRODAPINNO3 + OH	\rightarrow	MTO2	1.0E-30
MT-13	PRODAPINO3 + OH	\rightarrow	MTO2	1.0E-30

MT-14	PRODLIMOH + OH	\rightarrow	MTO2	1.0E-30
MT-15	PRODLIMNO3 + OH	\rightarrow	MTO2	1.0E-30
MT-16	PRODLIMO3 + OH	\rightarrow	MTO2	1.0E-30
MT-17	MTKETONE + OH	\rightarrow	MTO2	1.0E-30
MT-18	MTO2H + OH	\rightarrow	MTO2	1.0E-30

Table S2-3: MEGAN 3 to CityChem compound mapping. SESQ in CB05 are same in CityChem. but currently not included in the chemistry mechanism. All Light-Dep (LDF=1) and all fast-reacting monoterpenes MT are allocated to limonene.

No.	MEGAN v3 species	CMAQ/CB05	CITYCHEM	No.	MEGAN v3 species	CMAQ/CB05	CITYCHEM
1	isoprene	ISOP	Isoprene	63	cadinene_g	SESQ	SESQ
2	MBO_2m3e2ol	IOLE	C3H6	64	nerolidol_t	SESQ	SESQ
3	pinene_a	TERP	APIN	65	bergamotene_b	SESQ	SESQ
4	pinene_b	TERP	APIN	66	bisabolene_a	SESQ	SESQ
5	myrcene	TERP	LIM	67	cedrol	SESQ	SESQ
6	ocimene_al	TERP	LIM	68	homosalate	SESQ	SESQ
7	ocimene_c_b	TERP	LIM	69	2ethyl_hexyl_salate	SESQ	SESQ
8	ocimene_t_b	TERP	LIM	70	cedrene_a	SESQ	SESQ
9	camphene	TERP	APIN	71	thujopsene	SESQ	SESQ
10	bornene	TERP	APIN	72	longifolene	SESQ	SESQ
11	fenchene_a	TERP	APIN	73	cadinol_a	SESQ	SESQ
12	tricyclene	TERP	APIN	74	zingiberene_a	SESQ	SESQ
13	carene_3	TERP	APIN	75	isolongifolene	SESQ	SESQ
14	fenchene_b	TERP	APIN	76	longicyclene	SESQ	SESQ
15	phellandrene_a	TERP	LIM	77	copaene_a	SESQ	SESQ
16	terpinene_g	TERP	LIM	78	bourbonene_b	SESQ	SESQ
17	terpinene_a	TERP	LIM	79	longipinene	SESQ	SESQ
18	limonene	TERP	LIM	80	cubebene_b	SESQ	SESQ
19	phellandrene_b	TERP	APIN	81	ylangene_a	SESQ	SESQ
20	terpinolene	TERP	LIM	82	cubebene_a	SESQ	SESQ
21	thujene_a	TERP	LIM	83	copaene_b	SESQ	SESQ
22	sabinene	TERP	LIM	84	kaur_16_ene	SESQ	SESQ

23	verbene	TERP	APIN	85	gurjunene_b	SESQ	SESQ
24	cymene_p	TERP	APIN	86	aromadendrene	SESQ	SESQ
25	cymene_o	TERP	APIN	87	methanol	MEOH	CH3OH
26	meta_cymenene	TERP	APIN	88	acetone	PAR	CH3COC2H5
27	p-cymenene	TERP	APIN	89	ethanol	ETOH	C2H5OH
28	camphor	TERP	APIN	90	acetaldehyde	ALD2	CH3CHO
29	bornyl_ACT	TERP	APIN	91	ethane	ETHA	C2H6
30	piperitone	TERP	APIN	92	ethene	ETH	C2H4
31	terpineol_a	TERP	APIN	93	propane	PAR	nC4H10
32	octanol	TERP	APIN	94	butene	OLE	C3H6
33	estragole	TERP	APIN	95	propene	OLE	C3H6
34	borneol	TERP	APIN	96	2_methylprop_1_ene	OLE	C3H6
35	thujone_b	TERP	APIN	97	butene_c2	IOLE	C3H6
36	thujone_a	TERP	APIN	98	butene_t2	IOLE	C3H6
37	terpineol_4	TERP	APIN	99	formaldehyde	FORM	HCHO
38	myrtenal	TERP	APIN	100	met_heptenone	ISPD	CH3COC2H5
39	fenchone	TERP	APIN	101	oxopentanal	ISPD	CH3CHO
40	octenol_1e3ol	TERP	APIN	102	geranyl_acetone	ISPD	APIN
41	ionone_b	TERP	APIN	103	hexanal	ISPD	CH3CHO
42	ipsenol	TERP	APIN	104	linalool	ISPD	LIM
43	caryophyllene_b	SESEQ	SESEQ	105	methacrolein	ISPD	MACR
44	caryophyllene_c_i	SESEQ	SESEQ	106	met_vinylketone	ISPD	MVKetone
45	cadinene_d	SESEQ	SESEQ	107	hexanol_1	ISPD	C2H5OH
46	bisabolene_b	SESEQ	SESEQ	108	cineole_1_8	ISPD	CH3COC2H5
47	farnescene_a	SESEQ	SESEQ	109	hexenal_t2	ISPD	CH3CHO
48	patchoulene_b	SESEQ	SESEQ	110	hexenol_c3	ISPD	C2H5OH
49	elemene_b	SESEQ	SESEQ	111	hexenal_c3	ISPD	CH3CHO
50	nerolidol_c	SESEQ	SESEQ	112	2met_nonatriene	ISPD	APIN
51	farnesol	SESEQ	SESEQ	113	methane	CH4	CH4
52	humulene_a	SESEQ	SESEQ	114	butanone_2	ISPD	CH3COC2H5
53	muurolene_a	SESEQ	SESEQ	115	terpinyl_ACT_a	ISPD	APIN
54	bergamotene_a	SESEQ	SESEQ	116	pentane	PAR	nC4H10

55	germacrene_B	SESQ	SESQ	117	hexane	PAR	nC4H10
56	selinene_b	SESQ	SESQ	118	decane	PAR	nC4H10
57	calarene	SESQ	SESQ	119	heptane	PAR	nC4H10
58	farnescene_b	SESQ	SESQ	120	undecane	PAR	nC4H10
59	acoradiene	SESQ	SESQ	121	tetradecene_1	PAR	nC4H10
60	humulene_g	SESQ	SESQ	122	carbon_monoxide	CO	CO
61	muurolene_g	SESQ	SESQ	123	nitric_OXD	NO	NO
62	germacrene_D	SESQ	SESQ				

Supplement S3 – Evaluation of modelled O₃ concentrations

Figure S3-1 shows time series of modelled vs. measured MDA8 O₃ concentrations at four measurement sites in Hamburg (13ST, 24FL, 51BF and 52NG) in the modelled period (April – October 2018) for the base and drought scenario, respectively. In addition to the time series, Figure S3-1 includes relevant statistical indicators (r, MB, RMSE – indicators are described in Supplement S6) for each scenario and station in the respective period. The correlation coefficient r ranges from 0.46 at 52NG to 0.79 at 13ST and 24FL. To the most extent, ozone concentrations are being underestimated by the model, which leads to a negative MB at 13ST, 51BF and 52NG. In contrast, at 24FL the MB has a positive value and both MB and RMSE reach their lowest values which indicates the best model performance compared to the other stations. It is noteworthy, that the differences between the statistical indicators of the base and drought scenario are negligible at all stations.

Table S3-1: Statistical evaluation of modelled maximum daily 8-hour rolling mean (MDA8) O₃ concentrations (based on hourly values) for each month and the scenarios base, drought and noBVOC under application of four available O₃ measurement sites in the study domain (Table S3-2).

site	month	scenario	n	FAC2	MB	MGE	NMB	NMGE	RMSE	r	COE	IOA
13ST	April	base	30	0.933	-19.972	20.687	-0.241	0.249	28.567	0.486	-0.317	0.342
13ST	April	drought	30	0.933	-19.973	20.687	-0.241	0.249	28.567	0.486	-0.317	0.342
13ST	April	noBVOC	30	0.933	-19.997	20.700	-0.241	0.250	28.589	0.485	-0.318	0.341
13ST	May	base	31	1.000	-27.709	27.824	-0.265	0.266	30.511	0.675	-1.077	-0.037
13ST	May	drought	31	1.000	-27.727	27.842	-0.266	0.267	30.529	0.675	-1.078	-0.037
13ST	May	noBVOC	31	1.000	-27.784	27.897	-0.266	0.267	30.583	0.676	-1.082	-0.039
13ST	June	base	30	1.000	-19.580	20.959	-0.224	0.240	24.838	0.800	-0.080	0.460
13ST	June	drought	30	1.000	-19.617	20.996	-0.224	0.240	24.866	0.801	-0.082	0.459
13ST	June	noBVOC	30	1.000	-19.647	21.026	-0.225	0.241	24.891	0.801	-0.083	0.458
13ST	July	base	31	0.968	-26.488	26.488	-0.287	0.287	31.320	0.762	-0.318	0.341
13ST	July	drought	31	0.968	-26.535	26.535	-0.287	0.287	31.366	0.763	-0.320	0.340
13ST	July	noBVOC	31	0.968	-26.560	26.560	-0.287	0.287	31.384	0.764	-0.321	0.339
13ST	August	base	31	0.935	-24.670	25.916	-0.287	0.301	32.373	0.710	-0.091	0.454
13ST	August	drought	31	0.935	-24.744	25.982	-0.288	0.302	32.453	0.710	-0.094	0.453
13ST	August	noBVOC	31	0.935	-24.777	26.004	-0.288	0.303	32.483	0.709	-0.095	0.453
13ST	September	base	30	0.933	-18.120	18.120	-0.260	0.260	20.382	0.778	-0.537	0.231

13ST	September	drought	30	0.933	-18.134	18.134	-0.260	0.260	20.396	0.778	-0.539	0.231
13ST	September	noBVOC	30	0.933	-18.166	18.166	-0.261	0.261	20.432	0.777	-0.541	0.229
13ST	October	base	31	0.935	-12.995	14.329	-0.246	0.272	16.873	0.770	-0.100	0.450
13ST	October	drought	31	0.935	-12.998	14.333	-0.246	0.272	16.876	0.770	-0.100	0.450
13ST	October	noBVOC	31	0.935	-13.005	14.339	-0.247	0.272	16.881	0.770	-0.101	0.450
24FL	April	base	30	0.933	11.155	22.326	0.143	0.286	27.387	0.402	-0.635	0.182
24FL	April	drought	30	0.933	11.154	22.325	0.143	0.286	27.388	0.402	-0.635	0.182
24FL	April	noBVOC	30	0.933	11.121	22.334	0.143	0.286	27.404	0.401	-0.636	0.182
24FL	May	base	31	1.000	10.369	13.354	0.101	0.130	15.795	0.800	0.084	0.542
24FL	May	drought	31	1.000	10.367	13.353	0.101	0.130	15.794	0.800	0.084	0.542
24FL	May	noBVOC	31	1.000	10.296	13.296	0.100	0.130	15.745	0.800	0.088	0.544
24FL	June	base	29	0.966	9.161	14.232	0.104	0.162	19.199	0.779	0.338	0.669
24FL	June	drought	29	0.966	9.134	14.215	0.104	0.162	19.189	0.779	0.339	0.669
24FL	June	noBVOC	29	0.966	9.086	14.188	0.103	0.161	19.178	0.779	0.340	0.670
24FL	July	base	31	1.000	2.635	14.668	0.027	0.153	17.683	0.786	0.319	0.659
24FL	July	drought	31	1.000	2.591	14.660	0.027	0.153	17.697	0.785	0.319	0.660
24FL	July	noBVOC	31	1.000	2.554	14.646	0.027	0.153	17.688	0.785	0.320	0.660
24FL	August	base	31	1.000	-0.111	13.666	-0.001	0.155	16.359	0.854	0.434	0.717
24FL	August	drought	31	1.000	-0.139	13.689	-0.002	0.155	16.381	0.853	0.433	0.716
24FL	August	noBVOC	31	1.000	-0.197	13.733	-0.002	0.156	16.418	0.852	0.431	0.716
24FL	September	base	30	1.000	1.901	10.074	0.026	0.138	12.575	0.689	0.246	0.623
24FL	September	drought	30	1.000	1.884	10.083	0.026	0.138	12.595	0.688	0.245	0.623
24FL	September	noBVOC	30	1.000	1.823	10.112	0.025	0.138	12.644	0.685	0.243	0.622
24FL	October	base	31	0.968	7.376	9.985	0.135	0.183	11.776	0.795	0.120	0.560
24FL	October	drought	31	0.968	7.375	9.985	0.135	0.183	11.776	0.795	0.120	0.560
24FL	October	noBVOC	31	0.968	7.369	9.988	0.135	0.183	11.780	0.795	0.120	0.560
51BF	April	base	30	0.933	-4.418	23.232	-0.052	0.275	28.353	0.281	-0.604	0.198
51BF	April	drought	30	0.933	-4.418	23.233	-0.052	0.275	28.353	0.281	-0.604	0.198
51BF	April	noBVOC	30	0.933	-4.434	23.233	-0.052	0.275	28.356	0.281	-0.604	0.198
51BF	May	base	31	1.000	5.075	11.733	0.048	0.111	13.970	0.780	0.200	0.600
51BF	May	drought	31	1.000	5.072	11.730	0.048	0.111	13.969	0.780	0.200	0.600
51BF	May	noBVOC	31	1.000	5.018	11.702	0.047	0.110	13.942	0.780	0.202	0.601
51BF	June	base	30	1.000	-5.200	12.165	-0.058	0.135	16.808	0.847	0.398	0.699
51BF	June	drought	30	1.000	-5.219	12.163	-0.058	0.135	16.819	0.846	0.398	0.699
51BF	June	noBVOC	30	1.000	-5.264	12.145	-0.058	0.135	16.831	0.846	0.399	0.700
51BF	July	base	31	1.000	-14.202	17.791	-0.143	0.180	22.751	0.752	0.205	0.603
51BF	July	drought	31	1.000	-14.223	17.809	-0.144	0.180	22.763	0.752	0.204	0.602
51BF	July	noBVOC	31	1.000	-14.263	17.837	-0.144	0.180	22.779	0.753	0.203	0.601
51BF	August	base	31	0.968	-16.391	18.748	-0.181	0.207	23.503	0.854	0.295	0.648
51BF	August	drought	31	0.968	-16.397	18.756	-0.181	0.207	23.512	0.854	0.295	0.647
51BF	August	noBVOC	31	0.968	-16.424	18.782	-0.181	0.207	23.543	0.853	0.294	0.647
51BF	September	base	30	0.967	-18.040	20.240	-0.239	0.268	23.974	0.716	-0.446	0.277

51BF	September	drought	30	0.967	-18.046	20.243	-0.239	0.268	23.979	0.716	-0.446	0.277
51BF	September	noBVOC	30	0.967	-18.076	20.260	-0.239	0.268	24.003	0.715	-0.448	0.276
51BF	October	base	31	0.903	-6.326	15.462	-0.110	0.268	17.494	0.497	-0.181	0.410
51BF	October	drought	31	0.903	-6.326	15.462	-0.110	0.268	17.495	0.497	-0.181	0.410
51BF	October	noBVOC	31	0.903	-6.328	15.463	-0.110	0.268	17.496	0.497	-0.181	0.410
52NG	April	base	30	0.933	-6.948	18.147	-0.081	0.211	23.883	0.523	-0.103	0.449
52NG	April	drought	30	0.933	-6.948	18.147	-0.081	0.211	23.883	0.523	-0.103	0.449
52NG	April	noBVOC	30	0.933	-6.989	18.178	-0.081	0.211	23.922	0.521	-0.105	0.448
52NG	May	base	31	0.968	-29.169	32.804	-0.266	0.299	37.731	-0.081	-1.284	-0.124
52NG	May	drought	31	0.968	-29.193	32.823	-0.266	0.299	37.757	-0.082	-1.285	-0.125
52NG	May	noBVOC	31	0.968	-29.259	32.854	-0.266	0.299	37.807	-0.082	-1.287	-0.126
52NG	June	base	30	0.967	-9.496	24.331	-0.102	0.261	30.975	0.078	-0.184	0.408
52NG	June	drought	30	0.967	-9.544	24.368	-0.103	0.262	31.020	0.076	-0.186	0.407
52NG	June	noBVOC	30	0.967	-9.602	24.389	-0.103	0.262	31.069	0.074	-0.187	0.407
52NG	July	base	31	0.968	-9.958	19.645	-0.103	0.204	25.791	0.303	-0.021	0.489
52NG	July	drought	31	0.968	-10.018	19.661	-0.104	0.204	25.811	0.303	-0.022	0.489
52NG	July	noBVOC	31	0.968	-10.050	19.676	-0.104	0.204	25.840	0.302	-0.023	0.489
52NG	August	base	31	1.000	-12.739	21.887	-0.134	0.231	27.663	0.552	0.054	0.527
52NG	August	drought	31	1.000	-12.786	21.925	-0.135	0.231	27.713	0.550	0.052	0.526
52NG	August	noBVOC	31	1.000	-12.808	21.937	-0.135	0.231	27.725	0.550	0.052	0.526
52NG	September	base	30	1.000	-5.353	15.916	-0.068	0.201	20.115	0.118	-0.108	0.446
52NG	September	drought	30	1.000	-5.368	15.929	-0.068	0.202	20.135	0.116	-0.109	0.445
52NG	September	noBVOC	30	1.000	-5.396	15.952	-0.068	0.202	20.163	0.115	-0.111	0.444
52NG	October	base	31	0.968	-3.858	10.507	-0.063	0.171	14.121	0.611	0.050	0.525
52NG	October	drought	31	0.968	-3.866	10.514	-0.063	0.171	14.125	0.611	0.049	0.525
52NG	October	noBVOC	31	0.968	-3.874	10.521	-0.063	0.171	14.131	0.611	0.049	0.524

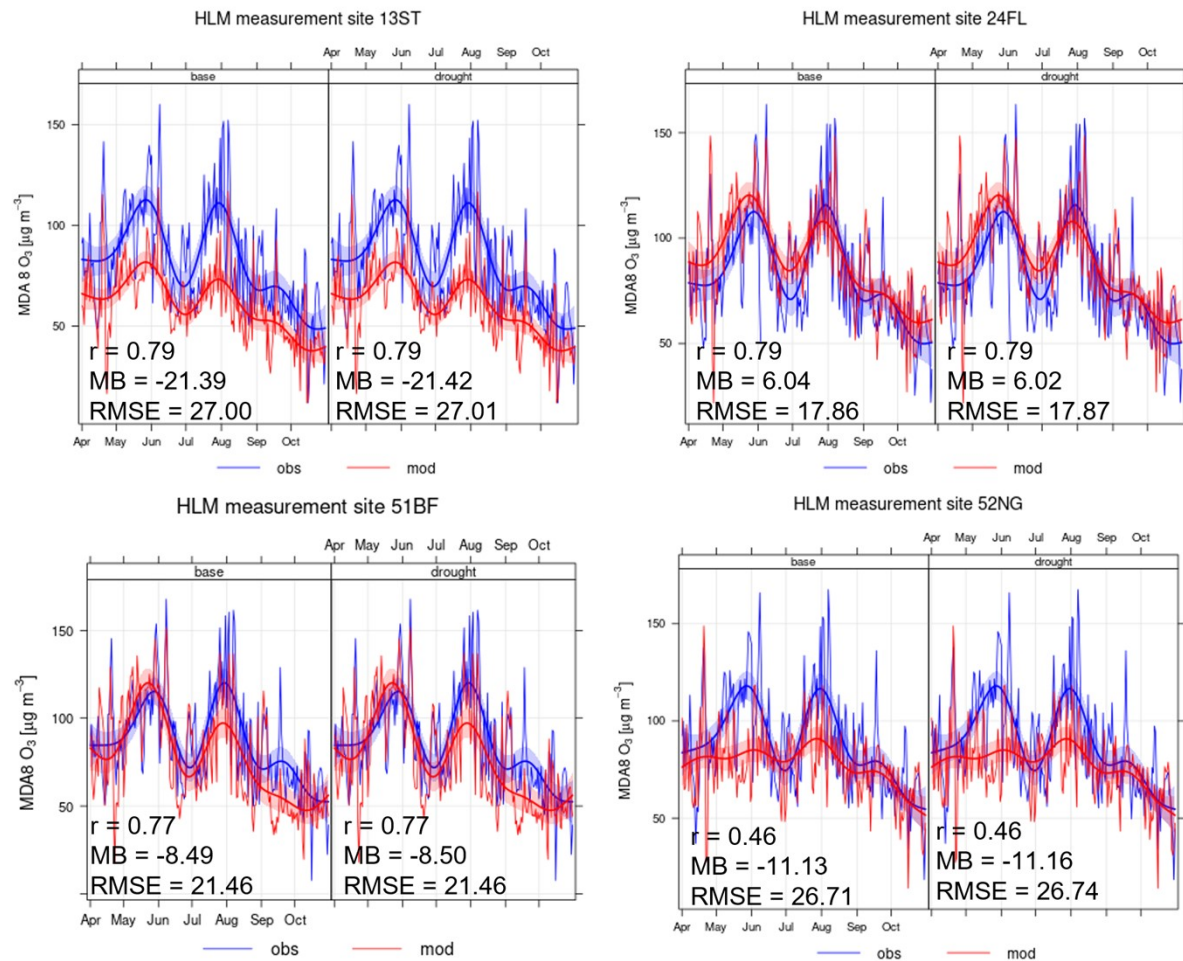


Figure S3-1: Time series of measured vs. modelled daily O₃ concentration at all available measurement sites in Hamburg for modelled period (April - Oct 2018) and both scenarios (without and with isoprene incl. stress).

Table S3-2: Hamburger Luftmessnetz (HaLM) O₃ measurement stations with type of stations and measured pollutants.

Station						
Code	Station Name	Station Type	Altitude	Lon	Lat	Pollutants Measured
13ST	Sternschanze	Urban	3.5	9.96834	53.56449	NO ₂ , O ₃ , PM10, PM2.5, SO ₂
51BF	Bramfeld	Urban	3.5	10.1105	53.63089	NO ₂ , O ₃
54BL	Blankenese	Background	3.5	9.786191	53.56806	NO ₂ , O ₃ , SO ₂
52NG	Neugraben	Background	3.5	9.857199	53.48098	NO ₂ , O ₃

Supplement S4 – Evaluation of modelled NO₂ concentrations

The time series evaluation of daily NO₂ (Figure S4-1) shows time series of modelled vs. measured NO₂ daily concentrations at four measurement sites in Hamburg (13ST, 24FL, 51BF and 52NG) in the modelled period (April – October 2018) for the base and drought scenario, respectively. In addition to the time series, Figure S4-1 includes relevant statistical indicators (r, MB, RMSE – indicators are described in Supplement S6) for each scenario and station in the respective period. The correlation coefficient r ranges from 0.53 at 52NG to 0.86 at 24FL. To the most extent, NO₂ concentrations are being underestimated by the model, which leads to a negative MB at all sites. Similar as for ozone, the statistical indicators reveal the best model performance at station 24FL. For NO₂ there are no differences between the statistics of the base and drought scenario.

Table S4-1: Statistical evaluation of modelled daily averaged NO₂ concentrations (based on hourly values) for each month and the scenarios base, drought and noBVOC under application of four available O₃ measurement sites in the study domain.

site	month	scenario	n	FAC2	MB	MGE	NMB	NMGE	RMSE	r	COE	IOA
13ST	April	base	30	0.667	-7.222	9.542	-0.291	0.385	11.307	0.644	-0.440	0.280
13ST	April	drought	30	0.667	-7.222	9.542	-0.291	0.385	11.307	0.644	-0.440	0.280
13ST	April	noBVOC	30	0.667	-7.226	9.539	-0.292	0.385	11.302	0.644	-0.440	0.280
13ST	May	base	31	0.548	-6.943	7.727	-0.415	0.462	8.813	0.610	-0.476	0.262
13ST	May	drought	31	0.548	-6.944	7.728	-0.415	0.462	8.814	0.610	-0.476	0.262
13ST	May	noBVOC	31	0.548	-6.946	7.730	-0.415	0.462	8.815	0.610	-0.476	0.262
13ST	June	base	30	0.667	-6.152	6.440	-0.394	0.412	7.388	0.735	-0.475	0.263
13ST	June	drought	30	0.667	-6.155	6.441	-0.394	0.412	7.389	0.735	-0.475	0.263
13ST	June	noBVOC	30	0.667	-6.160	6.444	-0.394	0.412	7.392	0.735	-0.475	0.262
13ST	July	base	31	0.581	-5.851	6.013	-0.383	0.393	7.152	0.782	-0.145	0.428
13ST	July	drought	31	0.581	-5.856	6.017	-0.383	0.394	7.156	0.782	-0.146	0.427
13ST	July	noBVOC	31	0.581	-5.861	6.021	-0.384	0.394	7.162	0.782	-0.146	0.427
13ST	August	base	31	0.742	-7.204	8.037	-0.337	0.375	9.611	0.672	-0.227	0.386
13ST	August	drought	31	0.742	-7.208	8.040	-0.337	0.376	9.614	0.672	-0.228	0.386
13ST	August	noBVOC	31	0.742	-7.212	8.040	-0.337	0.376	9.614	0.672	-0.228	0.386
13ST	September	base	30	0.567	-10.473	10.713	-0.383	0.391	11.961	0.846	-0.308	0.346
13ST	September	drought	30	0.567	-10.473	10.713	-0.383	0.391	11.961	0.846	-0.308	0.346
13ST	September	noBVOC	30	0.567	-10.475	10.714	-0.383	0.391	11.962	0.846	-0.308	0.346
13ST	October	base	31	0.677	-5.995	10.104	-0.199	0.336	11.633	0.858	0.234	0.617
13ST	October	drought	31	0.677	-5.995	10.105	-0.199	0.336	11.633	0.858	0.234	0.617
13ST	October	noBVOC	31	0.677	-5.997	10.105	-0.199	0.336	11.634	0.858	0.234	0.617
24FL	April	base	30	0.767	2.544	8.369	0.123	0.404	10.434	0.633	-0.350	0.325
24FL	April	drought	30	0.767	2.544	8.369	0.123	0.404	10.434	0.633	-0.350	0.325
24FL	April	noBVOC	30	0.767	2.541	8.367	0.123	0.403	10.431	0.633	-0.349	0.325
24FL	May	base	31	0.742	-4.099	4.812	-0.278	0.326	6.130	0.741	0.016	0.508
24FL	May	drought	31	0.742	-4.099	4.812	-0.278	0.326	6.131	0.741	0.016	0.508
24FL	May	noBVOC	31	0.742	-4.108	4.821	-0.279	0.327	6.138	0.741	0.014	0.507
24FL	June	base	29	0.931	-2.128	3.839	-0.169	0.305	4.651	0.631	-0.136	0.432
24FL	June	drought	29	0.931	-2.131	3.840	-0.169	0.305	4.652	0.631	-0.136	0.432

24FL	June	noBVOC	29	0.931	-2.146	3.848	-0.170	0.306	4.660	0.630	-0.138	0.431
24FL	July	base	31	0.839	-3.814	5.152	-0.259	0.349	6.077	0.653	-0.233	0.384
24FL	July	drought	31	0.839	-3.818	5.155	-0.259	0.349	6.081	0.653	-0.234	0.383
24FL	July	noBVOC	31	0.839	-3.833	5.157	-0.260	0.350	6.084	0.653	-0.234	0.383
24FL	August	base	31	0.935	-2.133	5.562	-0.110	0.288	7.063	0.582	0.084	0.542
24FL	August	drought	31	0.935	-2.138	5.564	-0.111	0.288	7.065	0.582	0.084	0.542
24FL	August	noBVOC	31	0.935	-2.150	5.560	-0.111	0.288	7.058	0.583	0.085	0.542
24FL	September	base	30	0.933	-0.716	4.243	-0.031	0.184	5.066	0.934	0.482	0.741
24FL	September	drought	30	0.933	-0.716	4.244	-0.031	0.184	5.066	0.934	0.482	0.741
24FL	September	noBVOC	30	0.933	-0.720	4.244	-0.031	0.184	5.067	0.934	0.482	0.741
24FL	October	base	31	0.968	-1.129	5.099	-0.041	0.183	6.228	0.955	0.596	0.798
24FL	October	drought	31	0.968	-1.128	5.100	-0.041	0.183	6.230	0.955	0.596	0.798
24FL	October	noBVOC	31	0.968	-1.131	5.099	-0.041	0.183	6.228	0.955	0.596	0.798
51BF	April	base	30	0.700	-6.045	6.103	-0.387	0.390	7.015	0.733	-0.655	0.172
51BF	April	drought	30	0.700	-6.045	6.103	-0.387	0.390	7.015	0.733	-0.655	0.172
51BF	April	noBVOC	30	0.700	-6.047	6.105	-0.387	0.390	7.015	0.733	-0.656	0.172
51BF	May	base	31	0.968	-0.331	2.257	-0.042	0.287	2.811	0.563	0.143	0.571
51BF	May	drought	31	0.968	-0.331	2.257	-0.042	0.287	2.811	0.563	0.143	0.571
51BF	May	noBVOC	31	0.968	-0.339	2.254	-0.043	0.286	2.810	0.564	0.144	0.572
51BF	June	base	30	0.867	-1.873	2.701	-0.246	0.355	3.624	0.547	0.096	0.548
51BF	June	drought	30	0.867	-1.874	2.701	-0.246	0.355	3.624	0.547	0.097	0.548
51BF	June	noBVOC	30	0.867	-1.884	2.703	-0.248	0.355	3.627	0.547	0.096	0.548
51BF	July	base	31	0.839	-0.799	2.521	-0.110	0.348	2.940	0.721	-0.007	0.496
51BF	July	drought	31	0.839	-0.800	2.523	-0.110	0.348	2.941	0.721	-0.008	0.496
51BF	July	noBVOC	31	0.839	-0.813	2.522	-0.112	0.348	2.935	0.721	-0.007	0.496
51BF	August	base	31	0.645	-4.057	5.168	-0.331	0.422	5.821	0.642	-0.557	0.222
51BF	August	drought	31	0.645	-4.057	5.170	-0.331	0.422	5.822	0.642	-0.557	0.221
51BF	August	noBVOC	31	0.645	-4.067	5.167	-0.332	0.422	5.816	0.642	-0.557	0.222
51BF	September	base	30	0.467	-7.674	8.730	-0.479	0.545	9.987	0.470	-0.447	0.277
51BF	September	drought	30	0.467	-7.674	8.730	-0.479	0.545	9.987	0.470	-0.447	0.277
51BF	September	noBVOC	30	0.467	-7.676	8.731	-0.480	0.546	9.988	0.471	-0.447	0.277
51BF	October	base	31	0.677	-4.299	7.037	-0.239	0.391	8.646	0.805	0.177	0.588
51BF	October	drought	31	0.677	-4.299	7.038	-0.239	0.391	8.647	0.805	0.176	0.588
51BF	October	noBVOC	31	0.677	-4.301	7.037	-0.239	0.391	8.646	0.805	0.177	0.588
52NG	April	base	30	0.567	-7.691	8.031	-0.500	0.523	10.787	0.438	-0.220	0.390
52NG	April	drought	30	0.567	-7.691	8.031	-0.500	0.523	10.786	0.438	-0.220	0.390
52NG	April	noBVOC	30	0.567	-7.695	8.030	-0.501	0.522	10.786	0.439	-0.220	0.390
52NG	May	base	31	0.355	-6.901	8.512	-0.480	0.592	10.010	0.167	-0.698	0.151
52NG	May	drought	31	0.355	-6.902	8.513	-0.480	0.593	10.011	0.167	-0.698	0.151
52NG	May	noBVOC	31	0.355	-6.904	8.514	-0.481	0.593	10.013	0.167	-0.698	0.151
52NG	June	base	30	0.767	-3.867	4.341	-0.397	0.445	5.938	0.734	0.191	0.596
52NG	June	drought	30	0.767	-3.871	4.343	-0.397	0.446	5.938	0.734	0.191	0.596

52NG	June	noBVOC	30	0.767	-3.875	4.343	-0.397	0.446	5.939	0.735	0.191	0.596
52NG	July	drought	31,000	0.516	-5.728	5.897	-0.516	0.531	7.828	0.582	-0.071	0.464
52NG	July	noBVOC	31,000	0.516	-5.731	5.898	-0.516	0.531	7.830	0.582	-0.071	0.464
52NG	August	base	31,000	0.645	-4.121	5.495	-0.369	0.491	7.213	0.386	-0.319	0.340
52NG	August	drought	31,000	0.645	-4.125	5.496	-0.369	0.492	7.214	0.386	-0.319	0.340
52NG	August	noBVOC	31,000	0.645	-4.127	5.496	-0.369	0.492	7.214	0.386	-0.320	0.340
52NG	September	base	30,000	0.733	-4.414	5.124	-0.352	0.409	6.101	0.585	-0.438	0.281
52NG	September	drought	30,000	0.733	-4.414	5.124	-0.352	0.409	6.102	0.585	-0.438	0.281
52NG	September	noBVOC	30,000	0.733	-4.415	5.124	-0.352	0.409	6.102	0.585	-0.438	0.281
52NG	October	base	31,000	0.677	-6.055	6.277	-0.395	0.409	8.284	0.732	0.024	0.512
52NG	October	drought	31,000	0.677	-6.055	6.277	-0.395	0.409	8.283	0.732	0.024	0.512
52NG	October	noBVOC	31,000	0.677	-6.053	6.275	-0.395	0.409	8.283	0.732	0.025	0.512

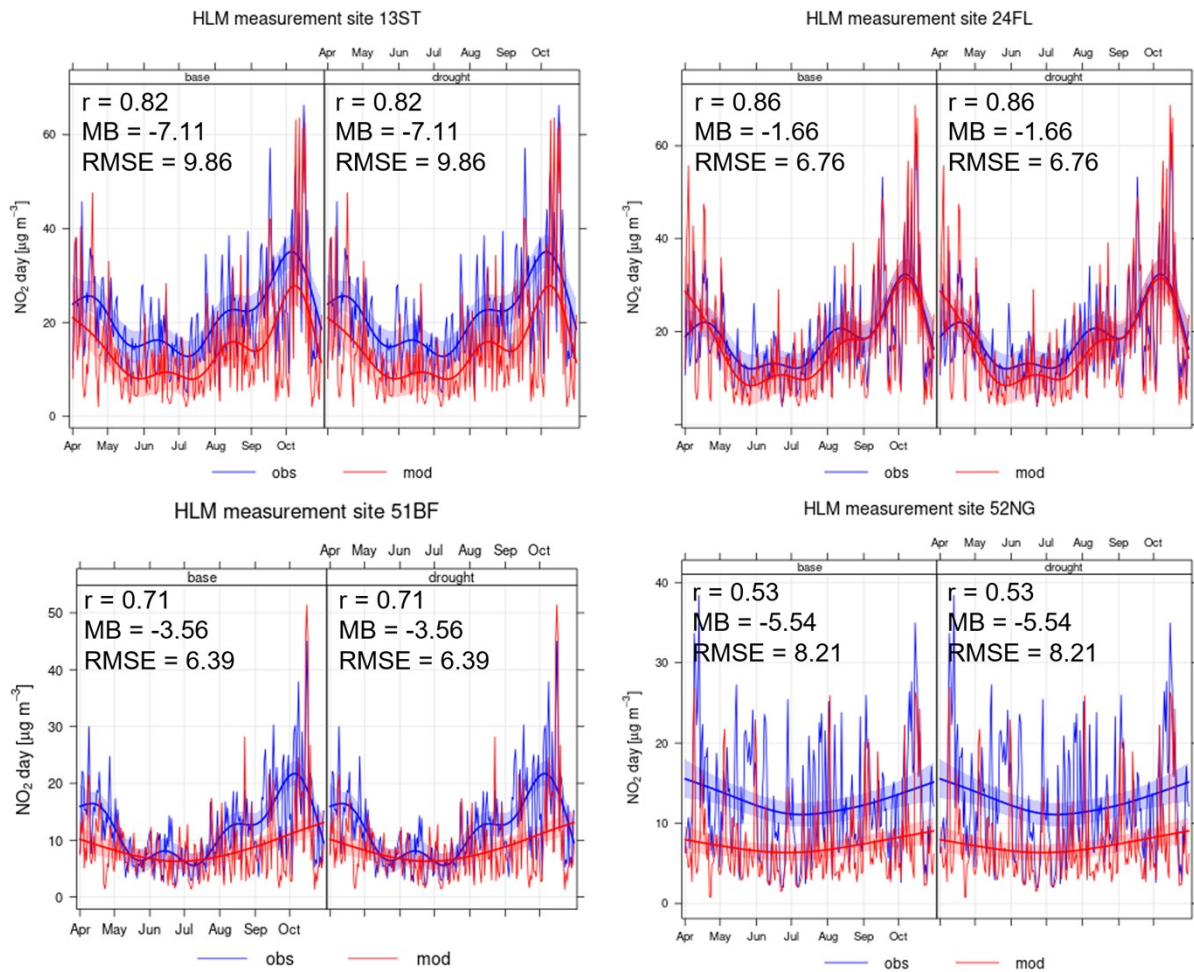


Figure S4-1: Time series of measured vs. modelled daily NO₂ concentration at the same measurement sites in Hamburg, which are available for NO₂, for modelled period (April - Oct 2018) and scenarios base and drought.

Supplement S5 – Evaluation of modelled meteorological parameters

Due to their importance, we added a performance evaluation of meteorological parameters, which are used to drive both, EPISODE-CityChem and MEGAN simulations. Table S5-1 depicts relevant statistical indicators for wind direction, wind speed, ground temperature, radiation, and rain at one available measurement site in the study domain (The Hamburg weather mast, <https://wettermast.uni-hamburg.de/>). The statistics indicate very good agreement of modelled meteorological variables with the measured values, with high correlations and low BIAS for wind direction, wind speed, temperature and radiation. The modelled precipitation has a high negation NMB of 0.6 for the modelled period, but matches the temporal distribution well.

Table S5-1: Statistical evaluation of modelled vs. measured daily meteorological parameters.

	<i>n</i>	FAC2	MB	NMB	NMGE	RMSE	<i>r</i>	COE	IOA
<i>WDIR</i>	213	0.93	-2.03	-0.01	0.18	50.89	0.80	0.36	0.68
<i>WSPD</i>	213	0.98	0.11	0.04	0.20	0.68	0.68	0.39	0.69
<i>TEMPG</i>	213	1.00	1.37	0.08	0.11	2.21	0.95	0.55	0.77
<i>RGRND</i>	213	0.95	8.73	0.05	0.16	45.91	0.87	0.61	0.81
<i>RAIN</i>	213	0.15	-0.03	-0.62	0.85	0.13	0.42	0.44	0.72

In addition to the statistics, we include here wind roses of the measured and modelled parameters to evaluate wind speed and direction at the same measurement site (Figure S5-1). In the modelled case, the highest frequency of winds originates from north-western directions while the observations reveal the highest frequency of winds to come from West and South-West. Furthermore, the model depicts relatively high-frequency winds from East and North-East which are not detectable in the observations. Overall, the mean wind speeds are well-matched between the modelled and observed cases.

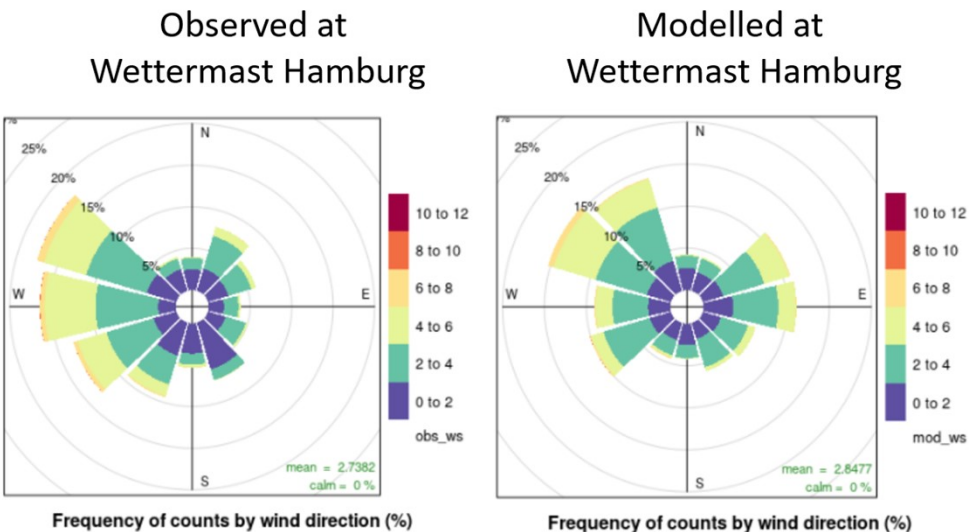


Figure S5-1: Wind roses of observed and modelled wind direction and wind speed at 10m height at weather mast Hamburg.

Furthermore, wind speed was evaluated as time series of the daily modelled vs. measured values at the Hamburg weather mast (Figure S5-2). The figure shows a satisfactory agreement between the modelled and the measured wind speed for both the range of values and their temporal variation.

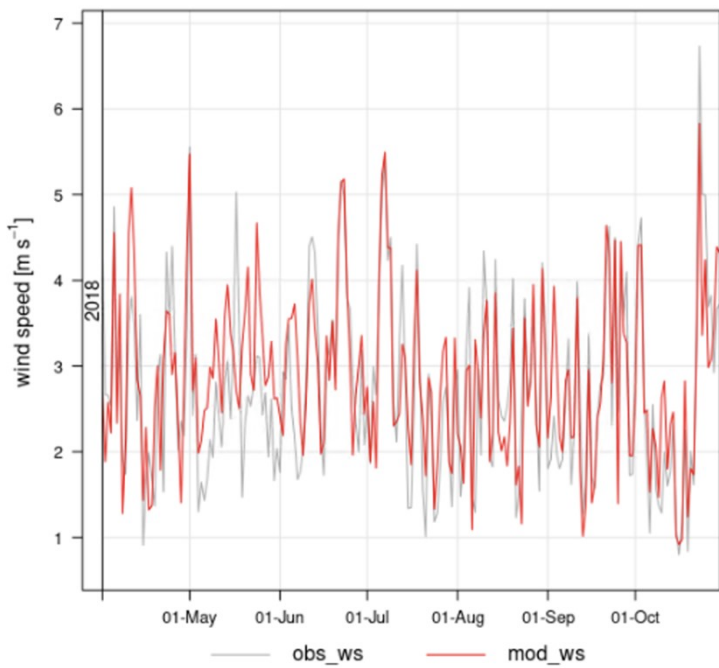


Figure S5-2: Observed vs. measured daily mean wind speed in 10m height at weather mast Hamburg.

Figure S5-3 shows the time series of modelled vs. measured ground temperature at Hamburg weather mast. The figure reveals a satisfactory agreement between the temporal variation in the modelled and the measured ground temperature. In the summer months June-August the model slightly overestimates the daily temperature peaks.

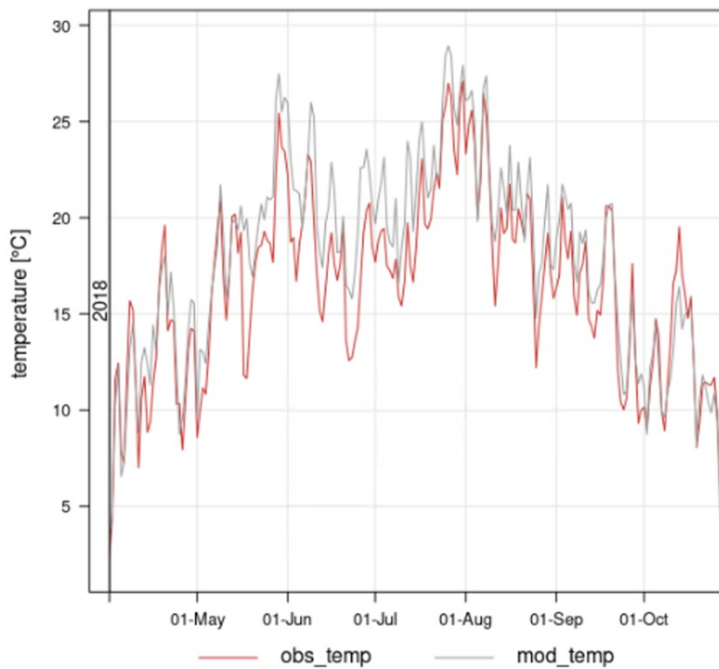
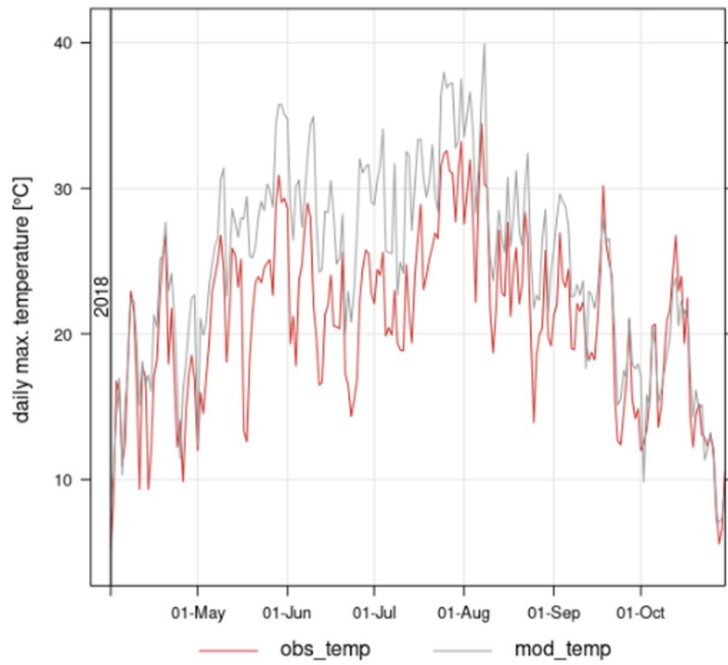


Figure S5-3: Observed vs. measured daily mean temperature in 10m height at weather mast Hamburg.

Additionally, in order to evaluate how well the hot conditions in the summer months were reproduced by the model, we add a figure showing the time series of modelled vs. measured maximum temperatures at the Hamburg weather mast (Figure S5-4). Again, the model slightly overestimates the daily temperature peaks in the summer months. Nevertheless, the temporal variations are matched well between the two cases.



FigureS5-4: Observed vs. measured daily max. temperature in 10m height at weather mast Hamburg.

Furthermore, we add a figure showing the time series of modelled vs. measured radiation at ground level at the Hamburg weather mast (Figure S5-5). As for the temperature, the timing of the peaks is well-matched although their values are sometimes overestimated and sometimes underestimated by the model.

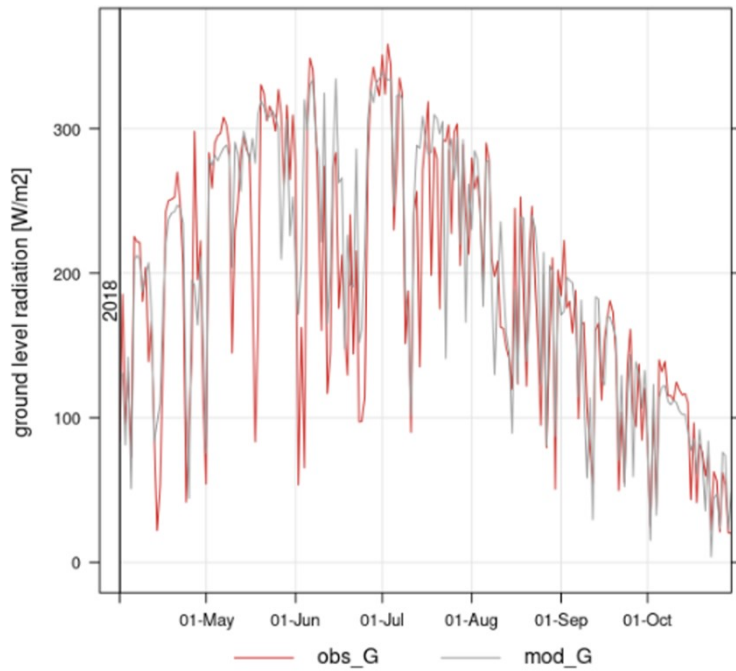


Figure S5-5: Observed vs. measured daily mean ground level radiation in at weather mast Hamburg.

To evaluate the model performance for precipitation we added time series of modelled vs. measured precipitation at the *Hamburg weather mast as well* (Figure S5-6). Although the timing of the modelled peaks is in good accordance with the observations, the model is not capable of reproducing extreme values as e.g., in the middle of July.

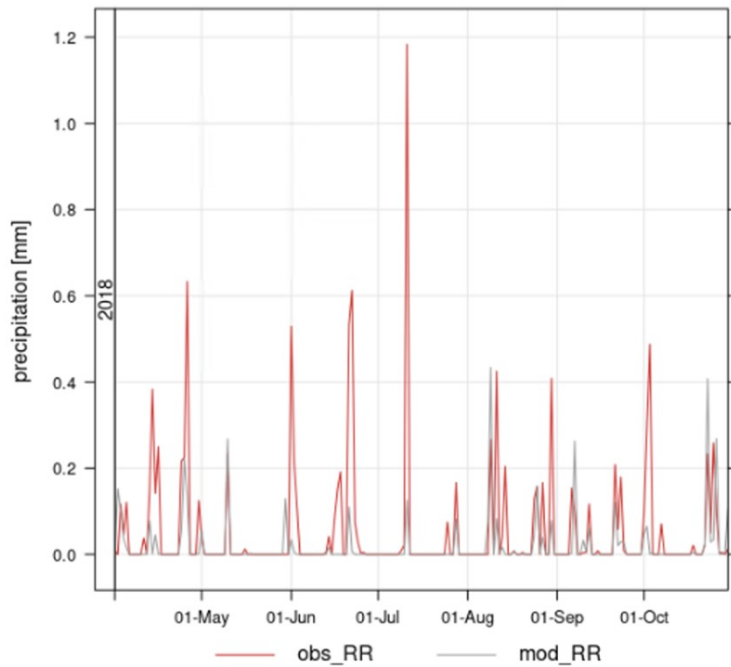


Figure S5-6: Observed vs. measured daily mean precipitation at weather mast Hamburg.

Finally, we wanted to evaluate the representation of drought in the meteorological input data. Therefore, we added the time series of the top layer soil moisture as an average of the study domain (Figure S5-7). In the vegetation period (April – August) the values frequently fell below a value of 20% which can be considered a very low soil moisture, indicating drought conditions. Accordingly, the modelled meteorological input is well-fitted to investigate drought stress on BVOC-emitting plants in the selected modeling period.

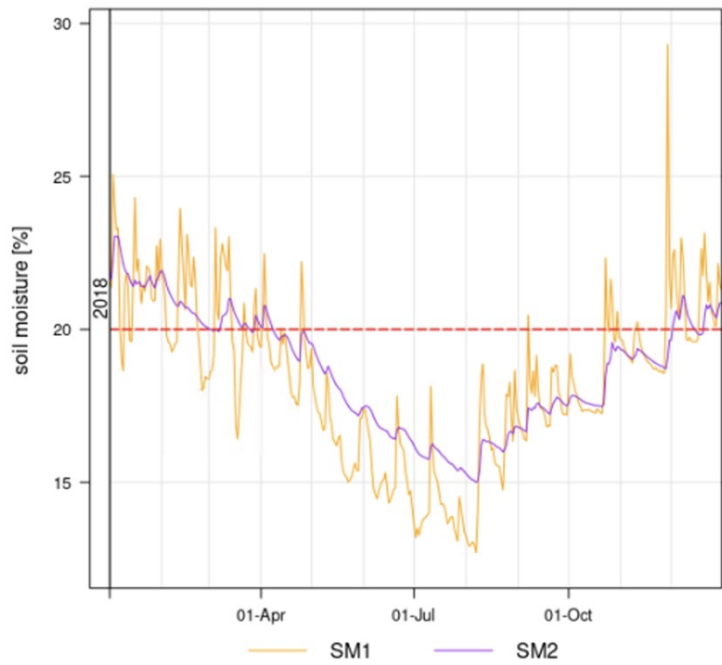


Figure S5-7: Modelled soil moisture in first and second level of ground layer in CCLM model simulations. The red dotted line indicates a value of 20% soil moisture, which can be used to identify a threshold for drought periods.

Supplement S6 - Statistical indicators and model performance indicators

In the statistical analysis of the model performance, the following statistical indicators are used: normalized mean bias (NMB), standard deviation (STD), root mean square error (RMSE), correlation coefficient (Corr), index of agreement (IOA) and the fraction of predictions within a factor of two of observations (FAC2). The overall bias captures the average deviations between the model and observed data and the NMB is given by:

$$NMB = \frac{\bar{M} - \bar{O}}{\bar{O}} \quad (1)$$

where \bar{M} and \bar{O} stand for the averaged model and observation results, respectively. The RMSE combines the magnitudes of the errors in predictions for various times into a single measure and is defined as

$$RMSE = \sqrt{\frac{1}{N} * \sum_{i=1}^N (M_i - O_i)^2} \quad (2)$$

where subscript i indicates the time step and N the number of observations. RMSE is a measure of accuracy, to compare prediction errors of different models for a particular data and not between datasets, as it is scale-dependent. The correlation coefficient (Pearson r) for the temporal correlation is defined as:

$$r = \frac{\sum_{i=1}^n (O_i - \bar{O}) \cdot (M_i - \bar{M})}{\sqrt{\sum_{i=1}^n (O_i - \bar{O})^2 \cdot \sum_{i=1}^n (M_i - \bar{M})^2}} \quad (3)$$

The index of agreement is defined as:

$$IOA = 1 - \frac{\sum_{i=1}^N (O_i - M_i)^2}{\sum_{i=1}^N (|M_i - \bar{M}| + |O_i - \bar{O}|)^2} \quad (4)$$

An IOA value close to 1 indicates agreement between modelled and observed data. The fraction of modelled values within a factor of two (FAC2) of the observed values are the fraction of model predictions that satisfy is defined as:

$$0.5 \leq \frac{M_i}{O_i} \leq 2.0 \quad (5)$$

For evaluation of modelled values in rural areas, the acceptance criteria is $FAC2 \geq 0.5$, while in urban areas it is $FAC2 \geq 0.3$ (Hanna & Chang, 2012).

Supplement S7 – CORINE LAND COVER 2018 land use classification

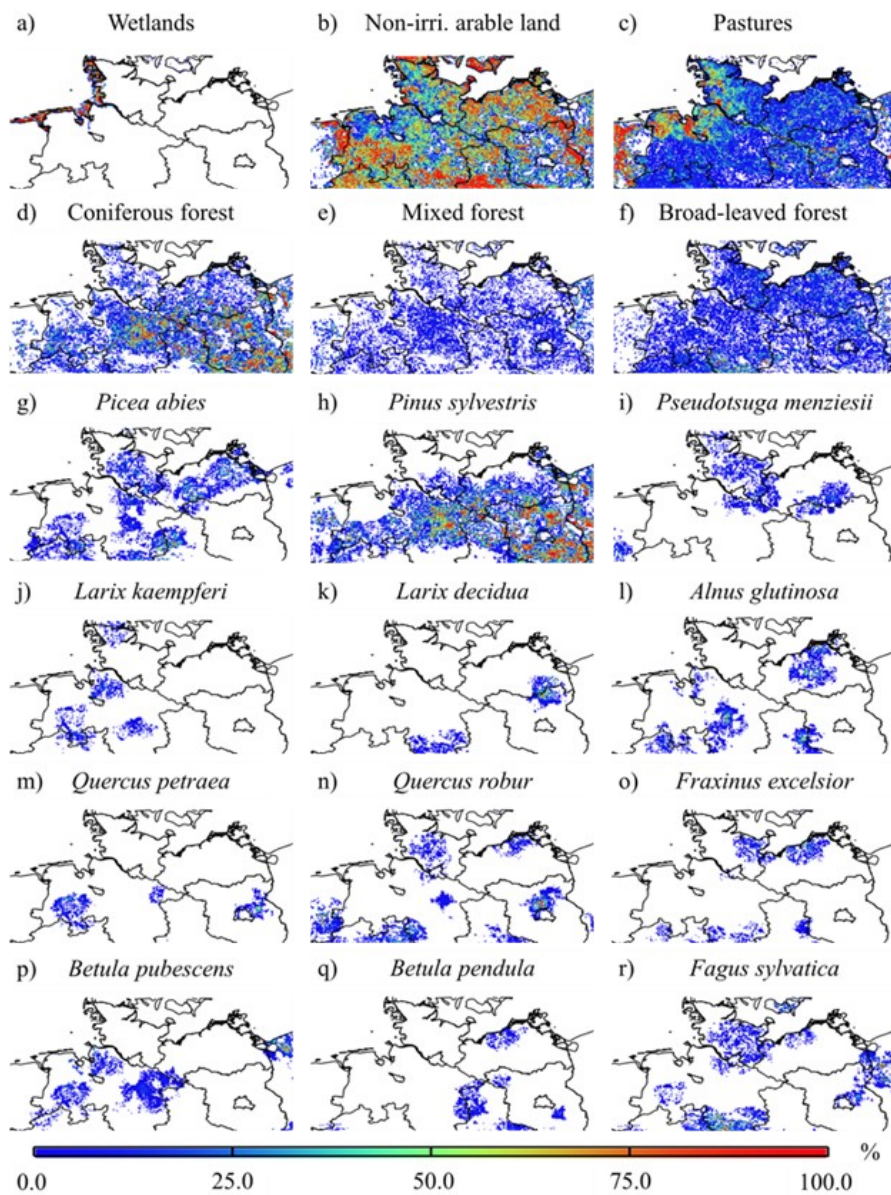
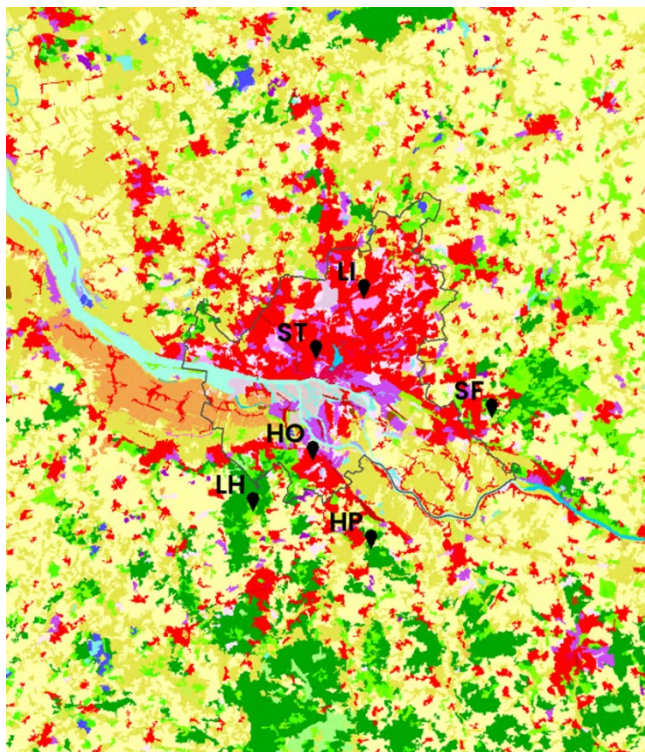


Fig. S7-1: Land use classification for northern Germany using CORINE2018 (<https://land.copernicus.eu/pan-european/corine-land-cover/clc2018>) for a)-f) and tree species information (Köble & Seufert 2001) for g)-r) on a $0.02^\circ \times 0.02^\circ$ grid.



111: Continuous urban fabric	321: Natural grasslands
112: Discontinuous urban fabric	322: Moors and heathland
121: Industrial or commercial units	323: Sclerophyllous vegetation
122: Road and rail networks and associated land	324: Transitional woodland-shrub
123: Port areas	331: Beaches, dunes, sands
124: Airports	332: Bare rocks
131: Mineral extraction sites	333: Sparsely vegetated areas
132: Dump sites	334: Burnt areas
133: Construction sites	335: Glaciers and perpetual snow
141: Green urban areas	411: Inland marshes
142: Sport and leisure facilities	412: Peat bogs
211: Non-irrigated arable land	421: Salt marshes
212: Permanently irrigated land	422: Salines
213: Rice fields	423: Intertidal flats
221: Vineyards	511: Water courses
222: Fruit trees and berry plantations	512: Water bodies
223: Olive groves	521: Coastal lagoons
231: Pastures	522: Estuaries
241: Annual crops associated with permanent crops	523: Sea and ocean
242: Complex cultivation patterns	
243: Land principally occupied by agriculture, with significant areas of natural vegetation	
244: Agro-forestry areas	
311: Broad-leaved forest	
312: Coniferous forest	
313: Mixed forest	

Figure S7-2: Corine Land Cover 2018 land use classes in MEGAN and EPISODE-CityChem modeling domains. © European Union, Copernicus Land Monitoring Service 2022, European Environment Agency (EEA).

Literature

Hanna, S.; Chang, J. Acceptance criteria for urban dispersion model evaluation. *Meteorol Atmos Phys* 2012, 116, 133–146, doi:10.1007/s00703-011-0177-1.

Kuenen, J., Dellaert, S., Visschedijk, A., Jalkanen, J.-P., Super, I., and Denier van der Gon, H.: CAMS-REG-v4: a state-of-the-art high-resolution European emission inventory for air quality modelling, *Earth Syst. Sci. Data*, 14, 491–515, <https://doi.org/10.5194/essd-14-491-2022>, 2022.

Ramacher, M.O.P.; Kakouri, A.; Speyer, O.; Feldner, J.; Karl, M.; Timmermans, R.; Denier van der Gon, H.; Kuenen, J.; Gerasopoulos, E.; Athanasopoulou, E. The UrbEm Hybrid Method to Derive High-Resolution Emissions for City-Scale Air Quality Modeling. *Atmosphere* 2021, 12, 1404. <https://doi.org/10.3390/atmos12111404>